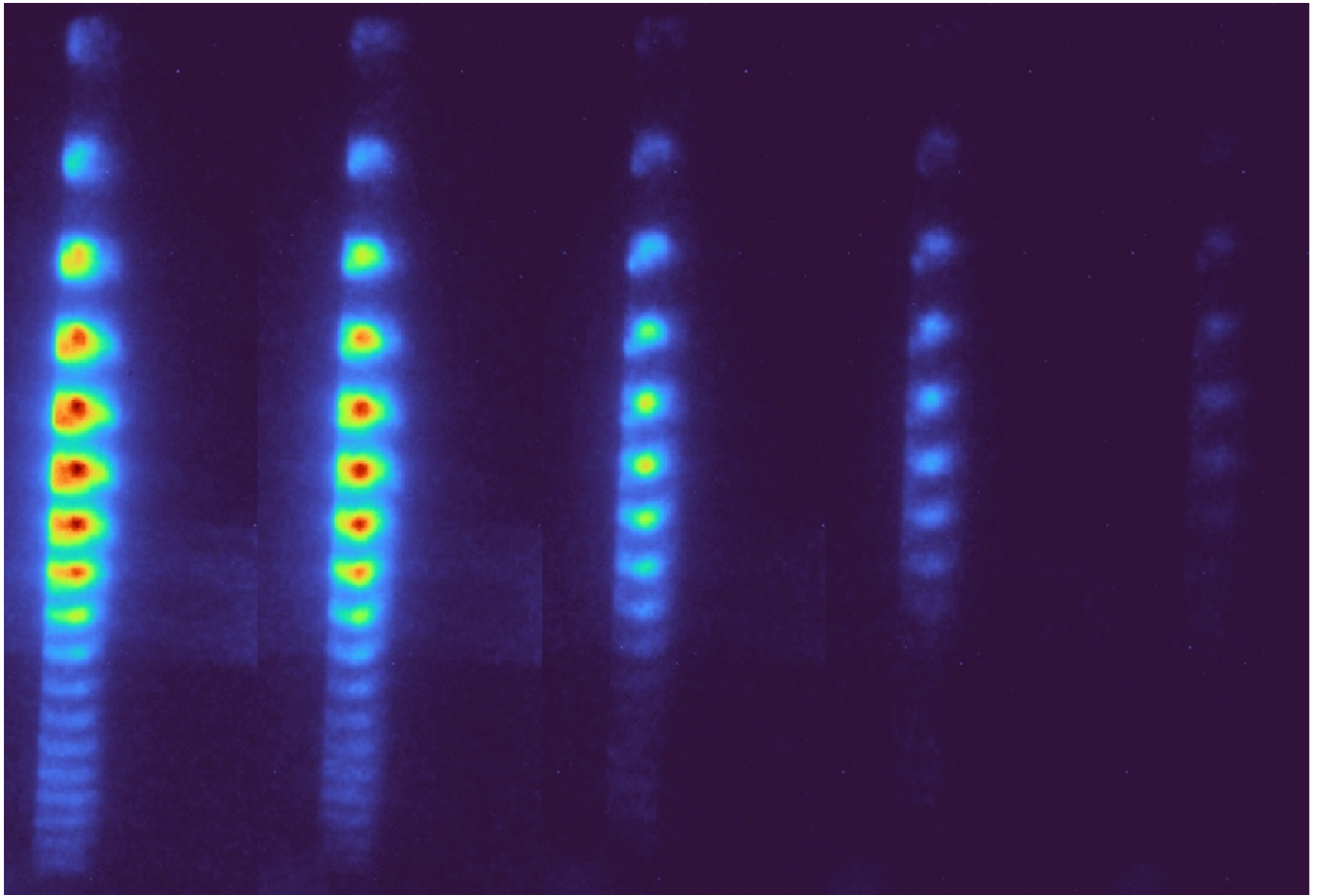




UNIVERSITY OF GOTHENBURG



The Effect of Pulse Duration, Laser Energy, and Gas Pressure on High Harmonic Generation Efficiency and Spectral Characteristics

Bachelor's thesis in Physics

Lukas Antonsson
Mulham Al Hashemi

Department of Physics

UNIVERSITY OF GOTHENBURG
Gothenburg, Sweden 2023

BACHELOR'S THESIS 2023

**The Effect of Pulse Duration, Laser Energy, and
Gas Pressure on High Harmonic Generation
Efficiency and Spectral Characteristics**

Lukas Antonsson

Mulham Al Hashemi

Advisors: Raimund Feifel, H el ene Coudert-Alteirac & Richard Squibb

Examiner: Martina Ahlberg



UNIVERSITY OF GOTHENBURG

Bachelor's in Physics

180 credits

Department of Physics

UNIVERSITY OF GOTHENBURG

Gothenburg, Sweden 2023

Abstract

This Bachelor's thesis investigates the role of pulse duration, laser energy, and gas pressure on the efficiency and colour of the High Harmonic Generation (HHG) process. HHG is a nonlinear optical phenomenon that generates extreme ultraviolet (XUV) radiation when an intense laser beam interacts with a material. XUV radiation is characterized by high photon energies and short wavelengths, making it useful for a wide range of applications in science and technology, such as imaging, spectroscopy, and microscopy.

The study is conducted using a laser system that generates femtosecond laser pulses, which are focused onto a gas target to generate XUV radiation. The energy and spectrum of the generated XUV radiation are analyzed for different values of pulse duration, laser energies, and gas pressure values, as well as the effects of using gas cells of different lengths and gap diameters.

The results show that changing the pulse duration and laser energy have a significant effect on the energy of the XUV photons and photon flux, while the gas pressure has a minor effect. Moreover, the use of gas cells of different lengths and gap diameters also affected the energy of the XUV photons and photon flux. The findings of this study have important implications for the design and optimization of HHG systems for various applications, including the development of more efficient and versatile XUV sources that can contribute to the advancement of various fields of science and technology.

Sammanfattning

Syftet med detta kandidatarbete var att undersöka hur pulslängd, laserenergi och gastryck påverkar effektiviteten och färgen hos processen Hög övertongenerering (HHG). HHG är en icke-linjär optisk process som genererar extrem ultraviolett (XUV) strålning när en högenergetisk laserstråle interagerar med vissa material. XUV-strålning karaktäriseras av hög fotonenergi och korta våglängder, vilket gör att den är användbar inom ett brett spektrum av tillämpningar inom naturvetenskap och teknologi, exempelvis bildbehandling, spektroskopi och mikroskopi.

Undersökningen genomfördes genom användning av ett lasersystem där pulser på femtosekunds-nivå genererades. Dessa pulser fokuserades sedan in i en gas där dessa XUV-pulser genererades. Dessa XUV-pulsers energier och spektran analyserades sedan för olika värden på pulslängd, laserenergi och gastryck, likaså undersöktes effekterna av att ha olika gasceller med varierande längder och diametrar.

Resultatet av denna undersökning visade att ändring av pulslängd och laserenergi hade en tydlig inverkan på energin hos dessa XUV-pulser. Gastrycket hade däremot en mindre tydlig påverkan. Även användandet av olika gasceller visade sig ha en påverkan på både energin hos XUV-fotonerna och fotonflödet. Resultatet av denna undersökning har viktiga följder inom design och optimering av HHG-system inom varierande tillämpningar. Detta inkluderar utvecklingen av mer effektiva och användbara XUV-källor som kan bidra till utvecklingen av olika fält inom naturvetenskap och teknologi.

Acknowledgements

I would like to thank the advisors Raimund Feifel and H el ene Coudert-Alteirac for all the help and support during this project. Without your help this thesis wouldn't have been as good as it has become.

I would also like to thank the examiner, Martina Ahlberg, for all the support you've given.

On a more personal level, I would like to thank my mother, father and brother for supporting me and believing in me. Their support has always helped me and I'm forever grateful that I have them in my life.

Lukas Antonsson, Gothenburg, May 2023

I would like to express my sincere gratitude to my advisors, Raimund Feifel and H el ene Coudert-Alteirac, for their invaluable support and guidance. Their expertise, constructive feedback, and encouragement have been instrumental in shaping and improving the quality of this thesis.

I would also like to thank Martina Ahlberg, my examiner, for her valuable comments and suggestions that helped me.

On the personal level, I would like to express my heartfelt gratitude to my wife and daughter for their unwavering support and encouragement throughout the time. I am forever grateful for their presence in my life.

I would also like to thank my father, mother, and sisters for their unending support, and belief in me. Their constant words of encouragement, love, and prayers have been a great source of strength to me.

Mulham Al Hashemi, Gothenburg, May 2023

Acronyms

Below is the list of acronyms that have been used throughout this thesis listed in alphabetical order:

| | |
|------|---------------------------------|
| CF | ConFlat |
| DFG | Difference Frequency Generation |
| FWHM | Full Width at Half Maximum |
| GDD | Group Delay Dispersion |
| HHG | High order Harmonic Generation |
| IP | Ionization Potential |
| IR | Infrared Radiation |
| KF | KleinFlansch (Small Flange) |
| MCP | Micro-Channel Plate |
| MPE | Maximum Permissible Exposure |
| NOHD | Nominal Ocular Hazard Distance |
| SFG | Sum Frequency Generation |
| SHG | Second Harmonic Generation |
| SPM | Self-Phase Modulation |
| THG | Third Harmonic Generation |
| XUV | Extreme Ultraviolet Radiation |

Contents

| | |
|--|-----------|
| Acronyms | xi |
| 1 Introduction | 1 |
| 2 Theory | 3 |
| 2.1 Linear and nonlinear optics | 3 |
| 2.2 Laser | 5 |
| 2.3 Femtosecond pulses | 7 |
| 2.4 High-order harmonic generation (HHG) and attosecond pulses | 9 |
| 2.5 Vacuum techniques | 12 |
| 2.6 Lab Safety | 12 |
| 3 Method | 15 |
| 3.1 Setup | 15 |
| 3.2 Procedure | 19 |
| 4 Results | 23 |
| 4.1 Pulse duration | 23 |
| 4.2 Laser energy | 26 |
| 4.3 Gas pressure | 28 |
| 4.4 Gas cells of different lengths and gap diameters | 29 |
| 4.5 Red and blue shift | 31 |
| 5 Conclusions | 33 |
| Bibliography | 35 |

1

Introduction

High Harmonic Generation (HHG) is a nonlinear optical phenomenon that occurs when an intense laser beam interacts with a material, leading to the generation of extreme ultraviolet (XUV) radiation. In recent years, the study of HHG has gained significant attention in the field of ultrafast optics, due to its potential for a wide range of applications in science and technology, such as imaging, spectroscopy, and microscopy. XUV radiation is characterized by high photon energies and short wavelengths, making it useful for studying the electronic and structural properties of materials on the atomic and molecular scale.

One of the key parameters that affect the HHG process is the pulse duration, which describes the temporal spreading of the laser pulse. The pulse duration has a significant impact on the energy and colour of the generated XUV radiation. Another important parameter is the laser energy, which determines the probability of ionization and recombination events occurring, and consequently affects the maximum photon energy generated in the HHG process. Additionally, gas pressure also has an impact on the energy of the generated XUV.

To better understand the fundamental parameters that affect the HHG process, it is essential to investigate the relationship between pulse duration, laser energy, and gas pressure on the efficiency and colour of the HHG process. In this Bachelor's thesis, we investigate the role of pulse duration, laser energy and pressure on the efficiency and colour of the HHG process. To this end, we use a laser system to generate femtosecond laser pulses, which are focused onto a gas target to generate XUV radiation. We analyze the energy and spectrum of the generated XUV radiation for different values of pulse duration, laser energies, and gas pressure values, as well as the effects of using gas cells of different lengths and gap diameters.

The findings of this study have important implications for the design and optimization of HHG systems for various applications. By understanding the fundamental parameters that affect the HHG process, we can develop more efficient and versatile XUV sources, which can contribute to the advancement of various fields of science and technology.

2

Theory

In the following sections, linear and nonlinear optics, laser, femtosecond pulses, high-order harmonic generation, vacuum techniques and lab safety are gone through.

2.1 Linear and nonlinear optics

Linear optics and nonlinear optics are two branches of optics that study the behavior of light in different materials and conditions.

Linear optics is the study of the behavior of light in materials that exhibit linear response to the incident electric field of light. This means that the optical properties of the material, such as its refractive index and absorption coefficient, do not depend on the intensity of the incident light. In other words, the optical response of the material is proportional to the incident electric field. Mathematically, this is described by the linear wave equation:

$$\nabla^2 \mathbf{E} - \mu\epsilon \frac{\partial^2 \mathbf{E}}{\partial t^2} = 0 \quad (2.1)$$

where \mathbf{E} is the electric field, μ is the magnetic permeability of the material, ϵ is the electric permittivity of the material, t is time and $\frac{1}{\sqrt{\mu\epsilon}} = c$ is the speed of the wave. In linear optics, the electric permittivity of the material is constant, and the electric field of the incident light propagates through the material without changing its properties [1].

On the other hand, nonlinear optics is the study of the behavior of light in materials that exhibit nonlinear response to the incident electric field of light. This means that the optical properties of the material depend on the intensity of the incident light, and the electric permittivity of the material becomes a function of the electric field [2].

In nonlinear optics, the electric permittivity of the material becomes a nonlinear function of the incident electric field, and the electric field of the incident light can interact with the material in a way that changes its properties.

In optics, the concept of polarization is often discussed. There are two different kinds of polarization. One kind is the polarization in a material. This works in the way that if you put a neutral atom in an electric field, \mathbf{E} , the atom is going

to be affected by the field although the atom itself is neutral. This is because the positively charged nucleus is moved in the direction of the field while the negatively charged electrons are moved in the other direction. This action induces a dipole in the material. But the attraction in the atom still tries to hold it together. The equilibrium between the two opposing forces leaves the atom polarized [3]. This kind of polarization can be expressed as:

$$\mathbf{P} = \epsilon_0 \sum_n \chi^{(n)} \mathbf{E}^n \quad (2.2)$$

where the $\chi^{(n)}$ -s are the n-th order susceptibilities of the material, which describe how the electric permittivity of the material changes as a function of the incident electric field and the $\mathbf{E}^{(n)}$ -s are the n-th order terms of the electric field.

Nonlinear optics is a fascinating field that studies light-matter interactions in materials that exhibit nonlinear responses to the incident electric field. The behavior of light in these materials is described by the nonlinear wave equation, which includes higher-order terms such as second-order, third-order, etc. When only the first-order susceptibility is considered, it is the linear optics that are being discussed ($n = 1$). However, when higher-order terms are included, nonlinear optics are obtained. Specifically, if the second-order terms, ($n = 2$), are included, $\chi^{(2)}$ -phenomena are discussed, which give rise to second harmonic generation (SHG), sum, and difference frequency generation (SFG/DFG). If the third-order terms, ($n = 3$) are included, $\chi^{(3)}$ -phenomena are discussed, which give rise to the optical Kerr effect, third harmonic generation (THG), and self-phase modulation (SPM) [4].

The $\chi^{(2)}$ -phenomena, such as SHG and SFG/DFG, arise from the nonlinear polarization induced in a material due to the interaction of two or more incident waves. The polarization induces a second harmonic wave or a sum/difference frequency wave, respectively. The efficiency of these processes is governed by the second-order susceptibility tensor $\chi^{(2)}$, which relates the induced polarization to the incident electric field.

The $\chi^{(3)}$ -phenomena, such as the optical Kerr effect, THG, and SPM, arise from the nonlinear refractive index induced in a material due to the interaction of the incident electric field with the medium. The induced refractive index modifies the propagation of the incident wave, resulting in a phase shift or frequency conversion. The efficiency of these processes is governed by the third-order susceptibility tensor $\chi^{(3)}$, which relates the induced refractive index to the incident electric field.

Second harmonic generation is a process where two photons of frequency ω combine to create a new photon with frequency 2ω . This process is a second-order phenomenon and is described by the second-order susceptibility $\chi^{(2)}$.

Sum frequency generation and difference frequency generation are other second-order phenomena, where two photons of different frequencies ω_1 and ω_2 combine to create a new photon with frequency $\omega_3 = \omega_1 + \omega_2$ or $\omega_3 = \omega_1 - \omega_2$, respectively.

Third harmonic generation is a third-order phenomenon where three photons of frequency ω combine to create a new photon with frequency 3ω . This process is described by the third-order susceptibility $\chi^{(3)}$ [2] [4].

The optical Kerr effect is an effect in nonlinear optical materials where the refractive index of the material changes due to the electric field of light.

The interaction between light and matter can result in a nonlinear optical effect known as Self-phase modulation (SPM). When an ultrashort light pulse traverses a medium, it induces a varying refractive index in the medium through the optical Kerr effect. This refractive index variation, in turn, causes a phase shift in the pulse, resulting in a modification of its frequency spectrum.

SPM holds significance in optical systems that rely on short and powerful light pulses, including lasers and optical fiber communication systems.

In contrast, linear optics deals with materials that exhibit linear response to the incident electric field of light. The behavior of light in these materials is described by the linear wave equation, which does not include higher-order terms. The electric permittivity of the material is constant, and the electric field of the incident light propagates through the material without changing its properties. Linear optics has many practical applications, such as in the design of optical devices and telecommunications systems.

2.2 Laser

A laser (Light Amplification by Stimulated Emission of Radiation) is a device that emits a highly concentrated and focused beam of light that has a narrow wavelength spectrum.

The concept of laser is based on the principles of quantum mechanics and the process of stimulated emission. According to these principles, energy can be absorbed by an atom or molecule and stored as an excited state. When the atom or molecule returns to its ground state, it releases this energy in the form of a photon (a particle of light). The laser concept involves amplifying this emission of light by stimulating the emission of many photons from a population of excited atoms or molecules [5].

The light generated by a laser is different from ordinary light in several ways. The laser beam is highly concentrated and focused, has a narrow range of wavelengths, and is highly collimated (meaning it does not diverge). The light produced by a laser is also coherent, meaning the waves are in phase with one another, which results in a highly directional and intense beam of light.

Light: All light is a form of electromagnetic radiation that is visible to the human eye.

Amplification: This is simply the process of making something bigger or more

2. Theory

powerful. When you turn up the volume on a radio, you are amplifying the sound; but with lasers, amplification makes the light brighter.

Stimulated: To stimulate means to stir to action. Laser light is created when a burst of light (electricity) excites the atoms in the laser to emit photons. These photons then stimulate the creation of additional identical photons to produce bright laser light.

Emission: The word "emission" refers to something that is sent out or given off. Stimulated laser emission consists of large numbers of photons that create intense laser light.

Radiation: Laser light is a form of energy that radiates, or moves out, from the laser source.

Lasers can be divided into different classes depending on how harmful they are to humans.

They range from class 1, which is "essentially" harmless to both eyes and skin, to class 4, which is very harmful to both eyes and skin.

The different classes of lasers are class 1, class 1M, class 2, class 2M, class 3R, class 3B and class 4.

Class 1 lasers are completely safe under normal use and normally have an output power of less than 0.4 mW. Examples of class 1 lasers are toys and many laser pointers. Class 1 can also include higher power lasers provided that they are either closed and sealed or have safety interlocks. Examples include DVD players and printers.

Class 2 lasers include only visible light lasers with a wavelength λ in the range of 400-700 nm. These are also safe to use due to the flash reflex. These have a power of between 0.4 - 1 mW of continuous light. However, intentionally looking at the beam of a class 2 laser can lead to eye damage.

Class 3R lasers are also said to be safe if handled correctly. For visible light, Class 3R lasers are limited to 5 mW of continuous wave radiation. These lasers can be dangerous under direct and reflective conditions but are normally not dangerous with diffuse reflections.

Class 3B lasers are dangerous and therefore must include both safety interlocks and a key switch. These lasers are more powerful than class 3R lasers but still have a power output of less than 500 mW. Class 3B lasers are dangerous under direct and reflective conditions, but are not normally dangerous under diffuse reflection. Examples of 3B lasers are those used in laser shows, but they are too powerful to be used as laser pointers. Lasers used in DVD players and printers would be classified

as 3B if they were removed from their respective devices.

Class 4 lasers have an output power of over 500 mW and are potentially very dangerous. The direct beam is a danger to both eyes and skin. Diffuse reflections from class 4 lasers can also be harmful. These lasers can also ignite combustible materials. Like class 3B lasers, these must include both safety interlocks and key switches. Many lasers used in science fall into this category, as do many medical lasers and lasers used to process materials.

Classes 1M and 2M have higher output power than their counterparts but are still safe to use as they often have both a larger beam diameter and greater beam divergence than their counterparts.

2.3 Femtosecond pulses

Femtosecond pulses are ultra-short pulses of light, typically lasting from a few femtoseconds (10^{-15} seconds) to several hundred femtoseconds. These pulses are generated using a variety of techniques, including mode-locked lasers, and optical parametric amplifiers.

One of the most significant applications of femtosecond pulse generation is in the study of ultrafast phenomena in physics. For example, femtosecond pulses have been used to investigate the dynamics of chemical reactions, the behavior of electrons in materials, and the interactions between light and matter. The ability to generate such short pulses of light has enabled researchers to probe the dynamics of these phenomena on their natural timescales, providing insights that were previously impossible to obtain.

The generation of femtosecond pulses is typically achieved using a mode-locked laser. In a mode-locked laser, the laser cavity is designed to allow the laser to oscillate at multiple frequencies simultaneously. The interaction between these frequencies results in the generation of a train of ultra-short pulses, with a repetition rate determined by the round-trip time of the laser cavity [6].

Another important aspect of femtosecond pulse generation is the control of the electric field of the pulses. The electric field of a light pulse describes the strength and direction of the oscillating electric field that accompanies the propagating light wave. The ability to control the electric field of femtosecond pulses is essential for many applications, including the generation of attosecond pulses and the manipulation of matter on ultrafast timescales [7].

A problem though with ultrashort pulses passing through a material is that the pulse disperses when it comes in contact with the material because of the difference in refractive index between the vacuum and the material. The refractive index is related to the speed of the wave according to the formula:

2. Theory

$$n = \frac{c}{v} \quad (2.3)$$

where c is the speed of light in vacuum and v is the wave speed in the material. Because of dealing with dispersive waves, the difference in speed between the colors is noticeable. This results in that the pulse is going to be spread out in time. Even though the waves spread out, in the end, it is important to arrive at the same time. This means the faster pulses have to take a longer path than the slower light. This means that they will arrive together. An example of this spreading can be seen in Figure 2.1.



Figure 2.1: The effect of dispersion. Taken from APE (Angewandte Physik und Elektronik), "Dispersion Compensation and Pulse Compression" article.

When discussing wave velocity, two different velocities can be considered. One is the group velocity v_g . That is the speed with which the envelope of the wave propagates. The phase velocity v_p is another aspect that can be discussed which is the speed with which the wave oscillates within the envelope. In the case of dispersive waves, the group velocity and the phase velocity differ. Figure 2.2 displays the various wave velocities.

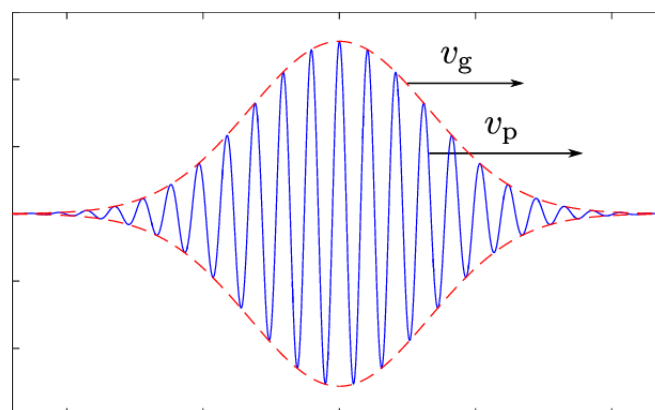


Figure 2.2: The phase and group velocity of a wave where the red curve is the envelope. Taken from Researchgate, "Mass polariton theory of light in dispersive media" article.

The shape of the electric field can be characterized by its pulse envelope.

Mathematically, the electric field at a given time t can be expressed as follows:

$$E(t) = A \cdot e^{-\frac{t^2}{4\sigma^2}} \cdot e^{-i\omega_0 t} \quad (2.4)$$

where ω_0 is angular frequency, A is normalization constant, and σ is transform-limited pulse of duration which is a pulse of a wave that has the minimum possible duration for a given spectral bandwidth.

The ability to generate ultra-short pulses of light and to control their electric field has enabled researchers to investigate ultrafast phenomena on their natural timescales, providing insights into the behavior of matter and electromagnetic radiation. Techniques such as mode-locked lasers, optical parametric amplifiers, and high-harmonic generation have enabled researchers to control the properties of femtosecond pulses, opening up new avenues for research and innovation in the fields of physics, chemistry, and biology.

2.4 High-order harmonic generation (HHG) and attosecond pulses

High-order harmonic generation (HHG) is a nonlinear optical process in which a high-intensity laser field interacts with an atom or molecule, resulting in the emission of high-energy photons in the form of harmonics of the fundamental frequency of the laser [8].

The three-step model is a theoretical framework that describes the physical mechanism of HHG [9]. It consists of the following steps, which can be seen in Figure 2.3.

1. Ionization: The first step is the ionization of an atom or molecule by the intense laser field. The laser field is strong enough to remove an electron from the atom or molecule, creating a positively charged ion and a free electron. This is done because the laser field "bends" the atomic potential which enables the electron to tunnel out from the atom.
2. Acceleration: The second step is the acceleration of the free electron by the laser field. The electron is accelerated away from the ion and gains energy from the laser field. Here the electric field changes direction which causes the potential to "bend" in the other direction.
3. Recombination: The third step is the recombination of the free electron with the ion. As the electron recombines with the ion, it releases its excess energy in the form of a high-energy photon. The energy of the photon is determined by the kinetic energy gained by the electron in the second step as well as the ionization potential (IP) of the atom.

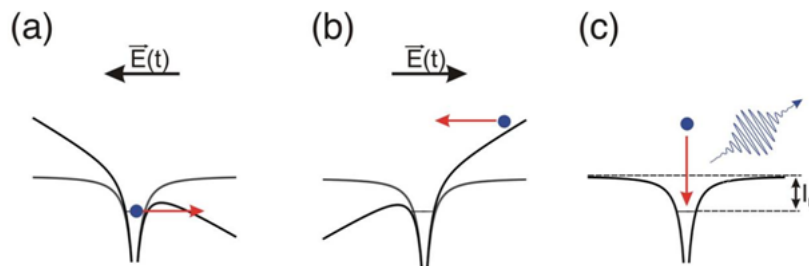


Figure 2.3: The three-step model that forms the basis for the HHG process. Taken from the University of Muenster, "High-order Harmonic Generation" article.

From Newton's second law it is possible to derive the trajectory and energy of the electron in step 2, since that step is a purely classical process. If we consider an electron at a specified time t_i just after tunneling with position $x(t_i) = 0$ and initial velocity $\dot{x}(t_i) = 0$. The electron is accelerated by a sinusoidal laser driving field with carrier frequency ω_0 and amplitude E_0 [10]. From Newton's law we get:

$$\ddot{x}(t) = -\frac{eE_0}{m_e} \sin(\omega_0 t) \quad (2.5)$$

where e is the elementary charge and m_e is the electron mass. If we integrate this with respect to time we get:

$$\dot{x}(t) = \frac{eE_0}{m_e \omega_0} [\cos(\omega_0 t) - \cos(\omega_0 t_i)] \quad (2.6)$$

and:

$$x(t) = \frac{eE_0}{m_e \omega_0^2} [\sin(\omega_0 t) - \sin(\omega_0 t_i) - \omega_0(t - t_i)\cos(\omega_0 t_i)] \quad (2.7)$$

The trajectories (Eq. 2.7) that are possible are displayed in Figure 2.4 a). Not all of the electrons that leave the atom will return. The kinetic energy for a specific trajectory can also be calculated as a function of ionization time t_i and return time t_r :

$$E_{kin} = \frac{1}{2} m_e \dot{x}^2(t_r) = \frac{e^2 E_0^2}{2 m_e \omega_0^2} [\cos(\omega_0 t_r) - \cos(\omega_0 t_i)]^2 = 2U_p [\cos(\omega_0 t_r) - \cos(\omega_0 t_i)]^2 \quad (2.8)$$

Here, U_p is the ponderomotive energy, i.e. the mean energy for an electron that's oscillating in the driving field.

To get the return times, we solve $x(t_r) = 0$, i.e.

$$\sin(\omega_0 t_r) - \sin(\omega_0 t_i) - \omega_0(t_r - t_i)\cos(\omega_0 t_i) = 0 \quad (2.9)$$

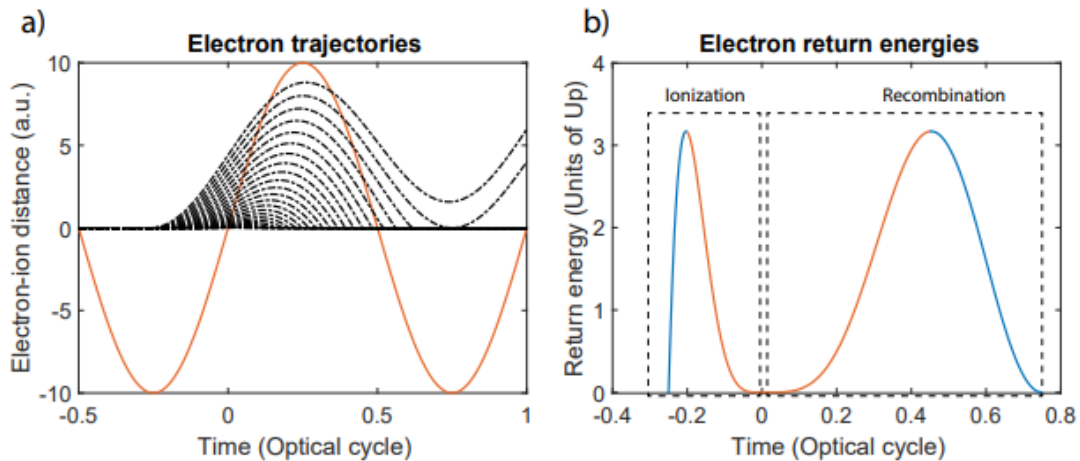


Figure 2.4: a) The possible trajectories for the electron. b) The electron return energies. Taken from [10].

The kinetic energy is displayed in Figure 2.4 b) as a function of the ionization time t_i and return time t_r . The energy of the emitted photon is $E = E_{kin} + I_p$ with I_p the ionization potential of the atom. Because of that, the maximum reachable energy is $E_{max} = 3.17U_p + I_p$. This is called the cut-off law which depends on the frequency ω_0 and on the laser intensity I because U_p is proportional to I [11].

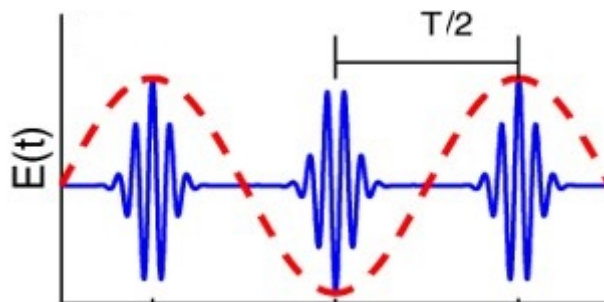


Figure 2.5: The attosecond pulses (in blue) generated by the laser field (in red).

It has been observed that ionization and recombination occur for every maximum and minimum of the electric field of the laser, resulting in the generation of XUV bursts every half period and forming a train of attosecond pulses separated by $T/2$, with T the laser period. And during the generation of attosecond pulses occurs the interference between them. These interferences give a spectral field of high harmonics spaced $2\omega_0$ apart. According to the Fourier transform, the more XUV pulses there are, the more discrete the harmonic spectrum of the pulse becomes. This is because the Fourier transform inverts the image, which means that if the pulses are separated in the space domain by $T/2$, in the frequency domain the distance between the pulses is going to be $2\omega_0$ [10].

For example, in an 800 nm ($T=2.6$ fs), the mid-period is 1.3 fs, which means that there is an attosecond pulse every 1.3 fs as shown in figure 2.5. This is also the

reason why we get distinct peaks rather than a continuous spectrum when plotting the pulses as a function of the frequency ω_0 [10].

Notably, this event occurs only when the laser's field is strong enough to ionize the atoms.

2.5 Vacuum techniques

Vacuum techniques play a crucial role in a wide range of scientific and industrial applications, including surface analysis, thin film deposition, and material synthesis. The need for a vacuum can be attributed to various factors.

Firstly, infrared (IR) radiation focused in air can create a plasma, which is undesirable in many experiments. Therefore, to prevent the formation of plasma, a vacuum is required to avoid any obstacles that could interfere with the propagation of the IR radiation.

Secondly, extreme ultraviolet (XUV) radiation is absorbed by air within just a few centimeters, thus requiring a vacuum to allow for the propagation of XUV radiation.

Lastly, the detection of electrons and ions should only come from the sample being analyzed, not from the surrounding air. Hence, a vacuum is necessary to avoid interference from air molecules during detection.

To create a vacuum, various types of pumps are employed, such as rotary pumps, turbo pumps, and differential pumps [12]. A combination of these pumps can achieve a vacuum pressure as low as 10^{-12} mbar, although a practical limit of 10^{-9} mbar is more commonly achieved in practice. The choice of materials used to bind the vacuum chamber's components together significantly affects the achievable vacuum pressure. Copper plates, for instance, can create a longer-lasting vacuum than rubber rings, albeit at a higher cost.

Contamination from grease or other materials on equipment can impede the vacuum creation process. Therefore, it is essential to clean the equipment thoroughly before use. Ultrasound cleaning can be used for a rough cleaning, while heat cleaning can provide a more thorough cleaning. Overall, vacuum techniques play a crucial role in scientific research and industrial applications, and a thorough understanding of these techniques is essential for success in these fields.

2.6 Lab Safety

* It is preferable that no one works alone in the laser laboratory.

* A warning light should be placed at the entrance of the laser laboratory, which lights up automatically with the operation of the laser device, to prevent people from suddenly entering the laboratory.

- * Warning signs should be placed in places exposed to laser radiation.
- * Determine the transmission direction of the laser beam inside the laboratory so that it does not interfere with the movement of people inside the laboratory.
- * The laser beam should be below eye level.
- * Goggles for each type of laser should be worn and a visual examination should be carried out every six months.

3

Method

In the upcoming sections the experimental setup and procedure is mentioned and explained.

3.1 Setup

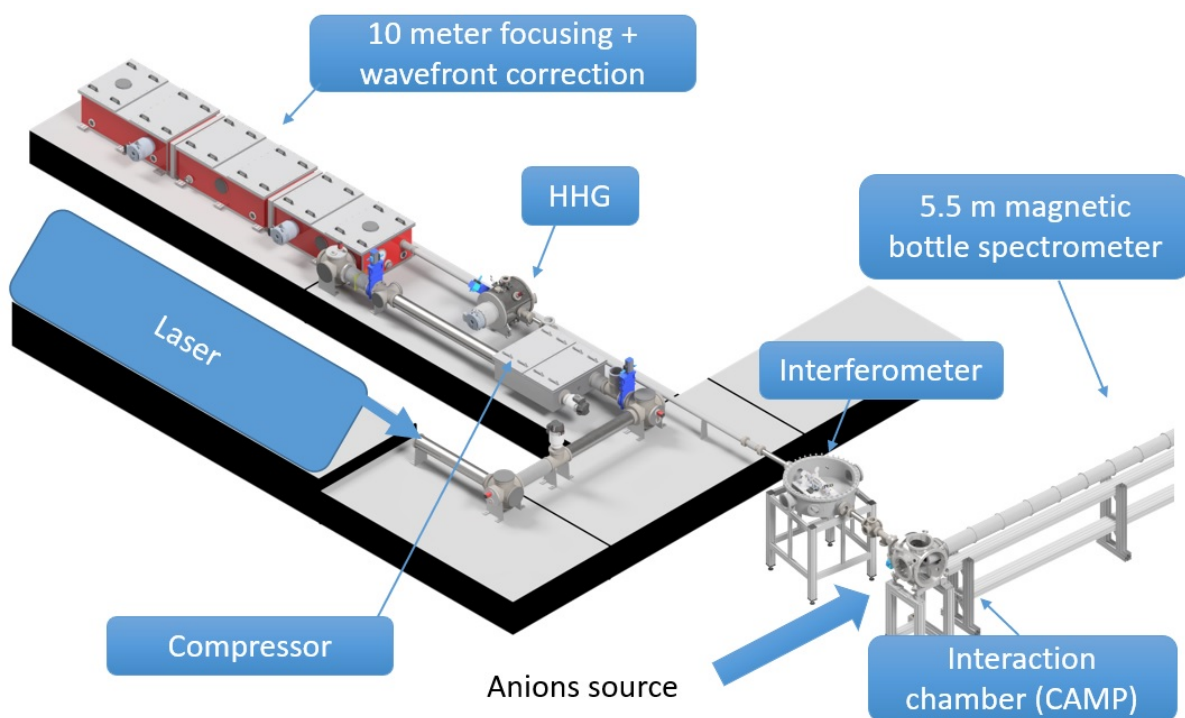


Figure 3.1: HHG setup in Attohallen.

The setup in Attohallen is based on creating an XUV pulse at attosecond intervals through an IR pulse as shown in figure 3.1 taking into consideration that in this experiment the anions source and related equipment were not installed and were replaced with the appropriate equipment. The chain to create this consists of transport to a compressor where the pulses are compressed in time. A common type of compressor setup is four pairs of chirped mirrors, which are arranged so that the laser pulse is incident on them at an angle. The chirped mirrors have a spatially varying reflectivity, which leads to a varying delay of the different frequency components of the pulse. By adjusting the spacing between the mirrors, the delay of

3. Method

each frequency component can be manipulated such that all the components arrive at the same time at the output of the compressor. This results in a shorter pulse duration with a higher peak power.

This is followed by focusing via ten meters mirrors towards to HHG chamber, with a gas like argon where harmonics are created. After that, a clearer vacuum is created via differential pumps and finally, the pulse meets a spectrometer where the image of the spectrum is analyzed via programs in LabView and Matlab.

First, a vacuum with a pressure of about 10^{-2} mbar is created by a rotary pump which is a type of rough pump and is used where large quantities of gas molecules are evacuated in a short period of time. It is used as a primary pump until it reaches pressure where other pumps can work more efficiently [12].

If a better vacuum is required, a turbo pump and a differential pump are used. A turbo pump takes down to 10^{-6} mbar. The highest vacuum is needed for example in the focusing and spectrometer where a turbo pump is used [12]. The turbopump can pull down to a lower pressure if better equipment is used, for example, to go between different materials a rubber ring (KF, KleinFlansch) can be used, which has the ability to reach 10^{-6} mbar and is reusable, or a copper ring (CF, ConFlat) which reaches 10^{-12} mbar at most but can only be used once as they are scratched and deformed during assembly as shown in figure 3.2.



Figure 3.2: (a)CF flange (b)KF flange

Following that, a differential pump is used which is a type of pump that is used in vacuum technology to maintain low pressure in a vacuum chamber. It works by creating a pressure difference between two chambers, with one having a higher pressure than the other [12]. The higher pressure chamber is connected to the inlet of the pump and the lower pressure chamber is connected to the outlet. The pressure difference causes gas molecules to flow from the high-pressure to the low-pressure chamber, which is pumped out of the system. This process is repeated continuously to maintain the desired level of vacuum in the chamber.

Vacuum may be more difficult to achieve with equipment that has come into contact with grease from hands or other dirty objects. The equipment should be washed first by ultrasound for rough cleaning and then by heat for a more thorough cleaning.

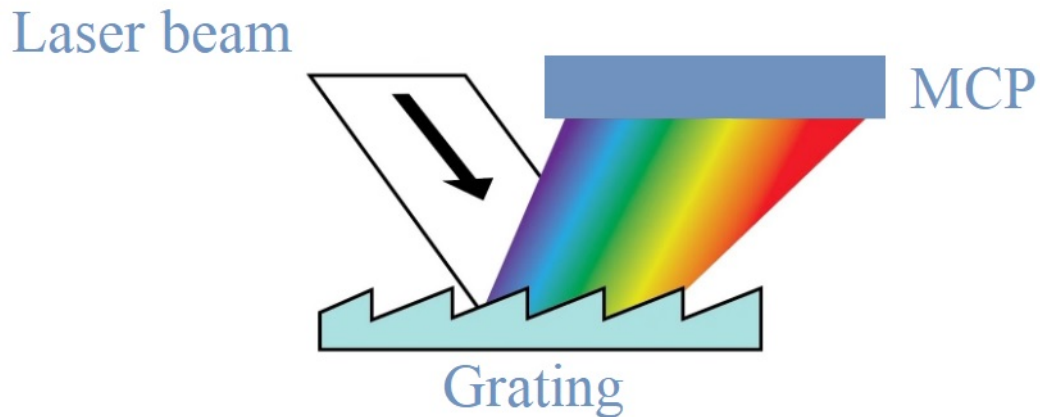


Figure 3.3: Laser beam through grating diffracts light, producing colors towards MCP.

Subsequently, a grating is used which is a surface with a series of closely spaced parallel grooves that can be used to diffract light. When a laser beam is directed through a grating, the different wavelengths of light are diffracted at different angles, producing different colours heading toward the MCP as shown in figure 3.3.

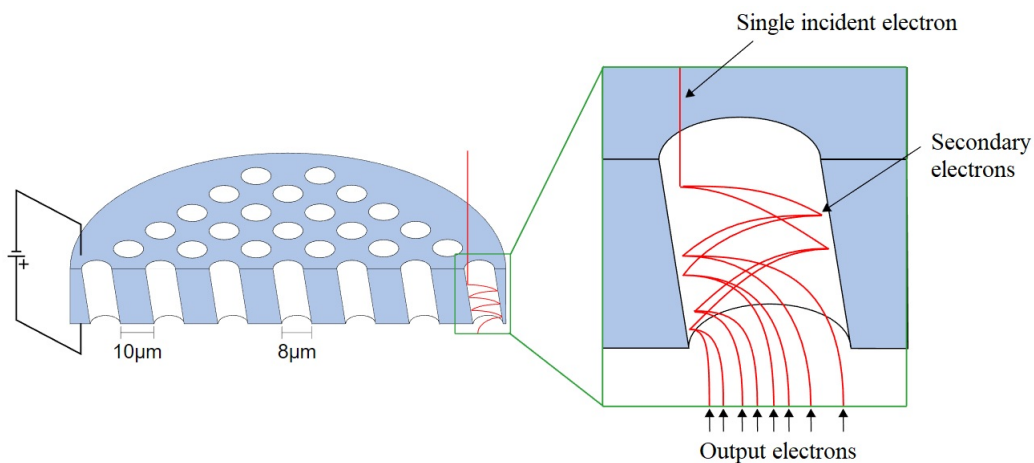


Figure 3.4: Schematic diagram of the operation of a microchannel plate. Image retrieved from Wikipedia, "Microchannel plate detector" article, and labeled as free to use without restrictions.

The MCP (Micro-Channel Plate) as shown in figure 3.4, is a type of electron multiplier that consists of a thin sheet with millions of tiny channels or holes,

3. Method

typically a few micrometers in diameter, etched or drilled through it [13]. These channels are arranged in a parallel or honeycomb pattern, and they are coated with a conductive material that uses secondary electron emission to amplify signals, which is employed in the experiment to amplify the electrons that hit the phosphorus screen and produce a visible image.

The principle of operation of an MCP is based on the secondary electron emission effect. When a high-energy electron or ion passes through one of the channels, it collides with the walls of the channel and generates several secondary electrons. These electrons are then accelerated towards the walls of the adjacent channels, where they produce more secondary electrons, and so on. This process creates a cascade of electrons that amplifies the original signal.

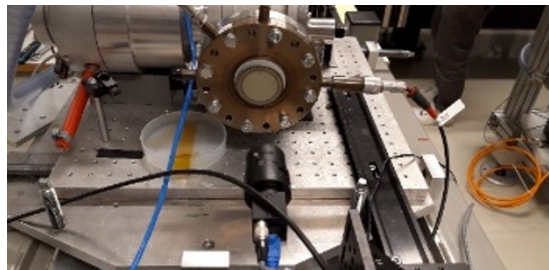


Figure 3.5: MCP and camera setup.

The amplified electrons from the MCP hit the phosphorus screen and produce a visible image, which can be captured by a camera (the detector) as shown in figure 3.5. The phosphorus screen is coated with a material that emits visible light (often green) when it is struck by electrons. The camera can be placed behind the phosphorus screen.

These pictures will be taken through the LabVIEW program, which enables the control of all equipment and the ability to change their values, and the program is used for automation, data acquisition, and analysis.

Later on, the images are processed and analyzed using MATLAB program (short for "matrix laboratory") which is a numerical computing environment and programming language developed by MathWorks. It allows users to perform a wide range of numerical computations and data analysis tasks, including matrix manipulations, statistical analysis, data visualization, and simulation.

Finally, figures containing spectra and 2D plots are obtained to analyze and find out the relationship between the different parameters that are significant for the experiment.

3.2 Procedure

The experiment was carried out to find out the relationship between changing pulse duration, laser energy, and gas pressure on the one hand, and the energy of the XUV photons and photon flux (the definition of photon flux is the number of photons per second per a unit area) on the other hand.

The experiment was also carried out using gas cells of different lengths and gap diameters.

Using LabVIEW, 50 images (frames) were taken and the time between frames was 1000 ms as shown in figure 3.6.

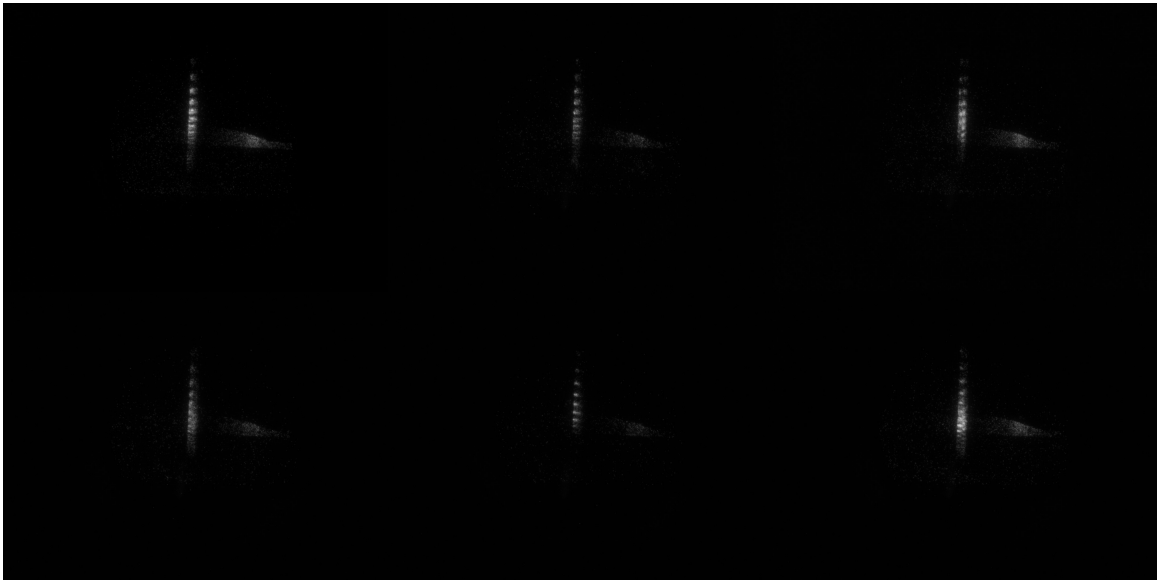


Figure 3.6: A random set of images.

In this study, a LabVIEW program was utilized to acquire 50 consecutive images (frames) for each variable or phase, with a time interval of 1000 ms. The experimental procedure commenced with the utilization of a cell of 1 cm length and 4 mm gap diameter. The LabVIEW program facilitated the manipulation of three parameters, namely pulse duration and that is through the group delay dispersion (GDD), laser energy, and gas pressure.

The initial parameter altered was pulse duration by altering the Group Delay Dispersion (GDD) which is a measure of the variation in group delay across different frequencies in a light pulse. Group delay refers to the time delay experienced by different frequency components of a light pulse as they propagate through a material or optical system. GDD is expressed in units of femtoseconds squared (fs^2) and is an important parameter in the design and characterization of ultrashort pulse lasers and other optical systems.

3. Method

GDD was initially set at $+300 \text{ fs}^2$, followed by incremental changes to $+250 \text{ fs}^2$, $+200 \text{ fs}^2$, and subsequently to -200 fs^2 , with 50 images captured at each GDD value. These values of the GDD together with the initial pulse duration of 13 fs at Full Width Half Maximum, (FWHM), gives a final pulse duration from 13 fs with $\text{GDD} = 0 \text{ fs}^2$ to 65 fs with $\text{GDD} = \pm 300 \text{ fs}^2$ at FWHM.

For given GDD , dispersed pulse length (final pulse duration) Δt is related to the initial pulse length (initial pulse duration) Δt_0 as:

$$\Delta t = \Delta t_0 \sqrt{1 + (4 \ln 2 \frac{GDD}{\Delta t_0^2})^2} \quad (3.1)$$

The only difference between $+300 \text{ fs}^2$ and -300 fs^2 is that the red and blue light comes in the other order.

The laser energy was subsequently varied in the range of 30 mJ to 50 mJ through the LabVIEW program, with 50 images taken for each energy value.

The gas pressure was subsequently adjusted within the range of 90 V to 200 V, with 50 images captured for each pressure value. Where the gas cell is injected with a gas such as argon and the amount of gas is controlled through a valve which is opening at 100 Hertz and then at a voltage of 100 Volts, the valve is only slightly opened, allowing a small quantity of gas to enter which leads to low gas pressure. In contrast, a voltage of 200 Volts significantly widens the valve, allowing for a substantially greater influx of gas leading to high gas pressure. Following this, the experimental procedure was repeated with three additional cells having lengths of 2 cm, 5 cm, and 5 cm, with gap diameters of 4 mm, 4 mm, and 5 mm, respectively.

The LabVIEW program facilitated the seamless alteration of these parameters during the experimental procedure facilitating the acquisition of comprehensive data and insights into the underlying physics of the experimental system.

Later on, a code was written using MATLAB to process and analyze the data and thus the ability to plot figures representing them.

In figure 3.7 at the top of the screen, is the lower photon energy, and by going down, the higher photon energy appears. And the spectrum of the photon energy which is obtained is shown also.

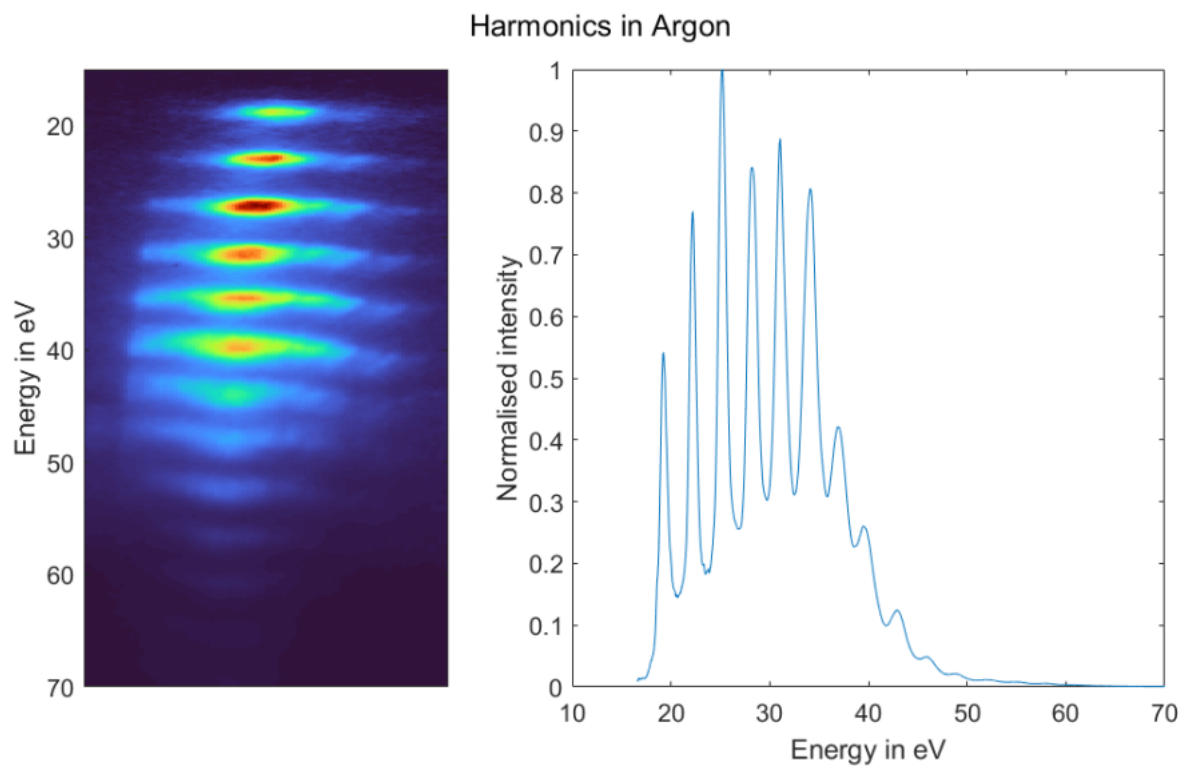


Figure 3.7: Harmonics in argon gas.

4

Results

In the following sections the results for the different parameters pulse duration, laser energy, gas pressure, different gas cells and red- and blueshift are presented.

4.1 Pulse duration

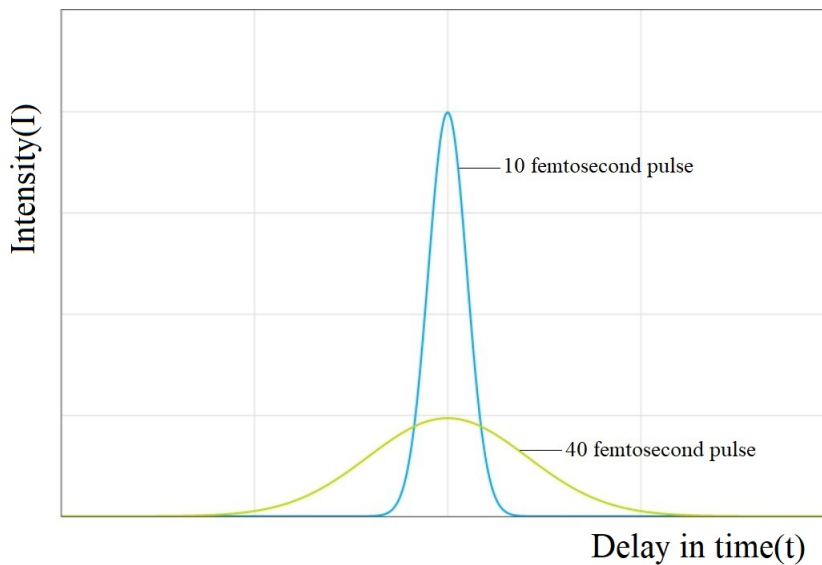


Figure 4.1: What happens if the 10 femtosecond pulse is stretched in time to 40 femtosecond.

Figure 4.1 shows 10 femtosecond pulse as intensity (I) is a function of delay in time (t) and what happens if the 10 femtosecond pulse is stretched in time to 40 femtosecond. In other words, the pulse duration is changed but the energy of the pulse when it is stretched stays the same.

The 40 femtosecond pulse is longer in time than the 10 femtosecond pulse and it has lower intensity but both of them have the same energy because the total energy is like what is under the curve.

The 40 femtosecond pulse has lower intensity and, in consequence, lower photon energy for the XUV, as is mentioned in the theory.

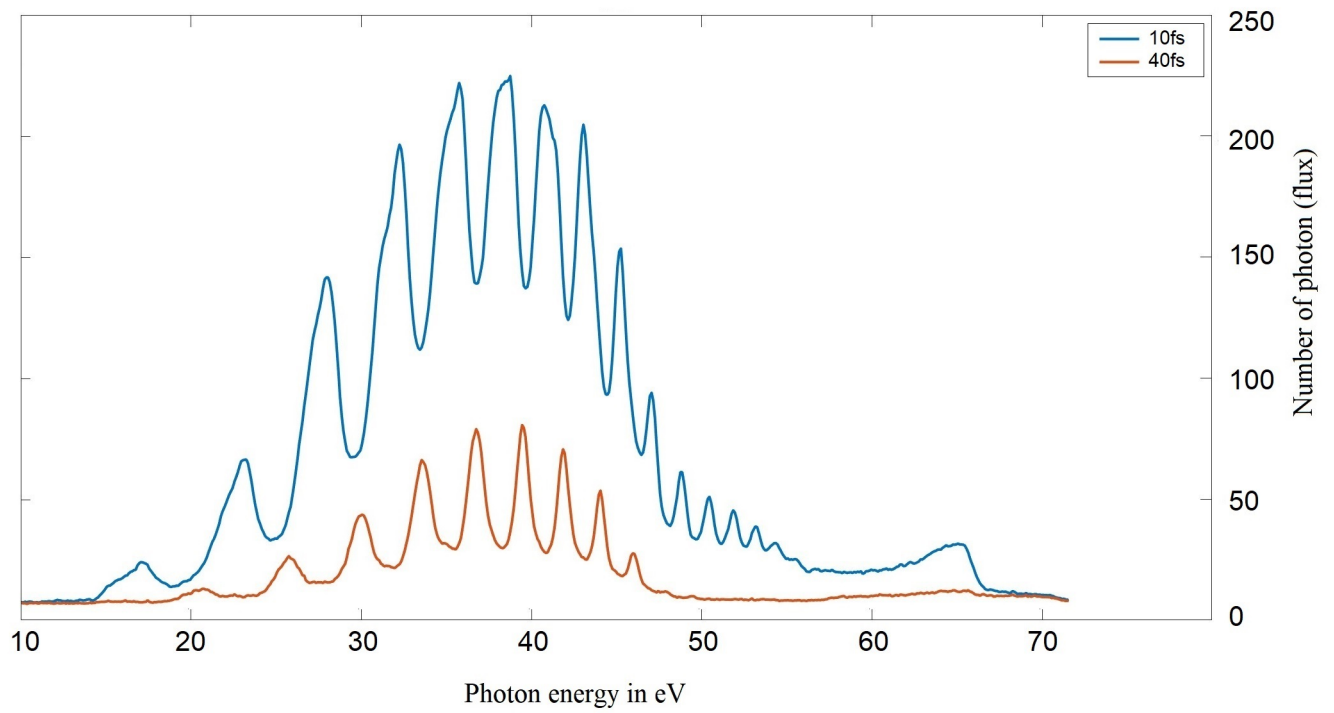


Figure 4.2: The spectrum for the same pulse energy but for different pulse duration.

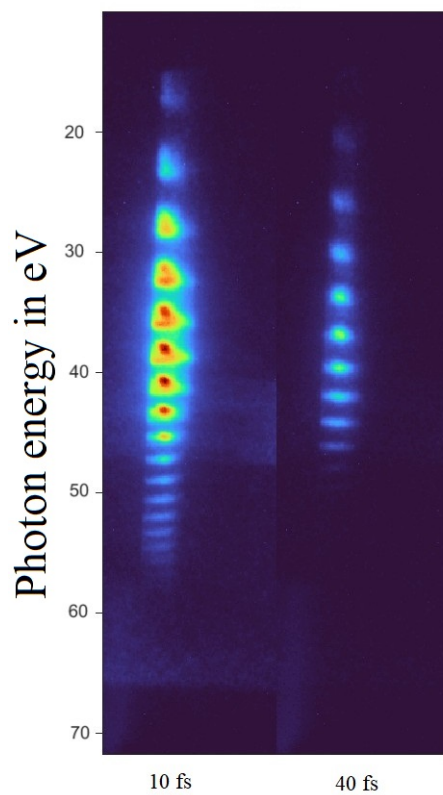


Figure 4.3: Harmonics for 10 femtosecond pulse and 40 femtosecond pulse

Therefore, if the spectrum is drawn as in figure 4.2 for the same pulse energy but

for different pulse duration; 10 femtosecond pulse and 40 femtosecond pulse, For the pulse of 40 femtosecond, lower photon energy peaks for the XUV will appear and it's lacking the higher energy peaks while higher photon energy peaks for the XUV will appear for the pulse of 10 femtosecond as can be seen also in figure 4.3. In addition to that, red spots are observed due to the number of XUV photons that are generated and then hit the detector and red spots become increasingly red as the number of XUV photons generated rises.

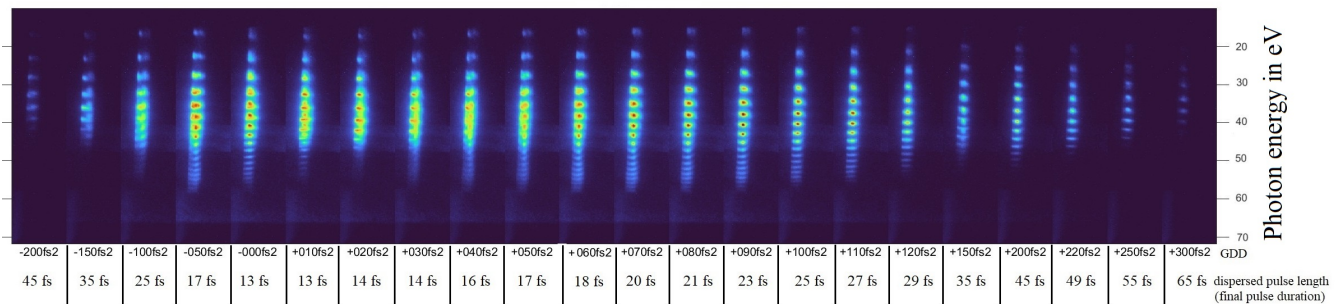


Figure 4.4: Harmonics for different values of pulse duration.

It is observed in figure 4.4 that the pulses are most compressed in the middle region and then the more dispersion added, the more pulses spread.

Because of that, at the top on the extreme right and the extreme left, pulses have lower intensity and then the number of peaks decreases in what is called “cut off” the highest peak.

4.2 Laser energy

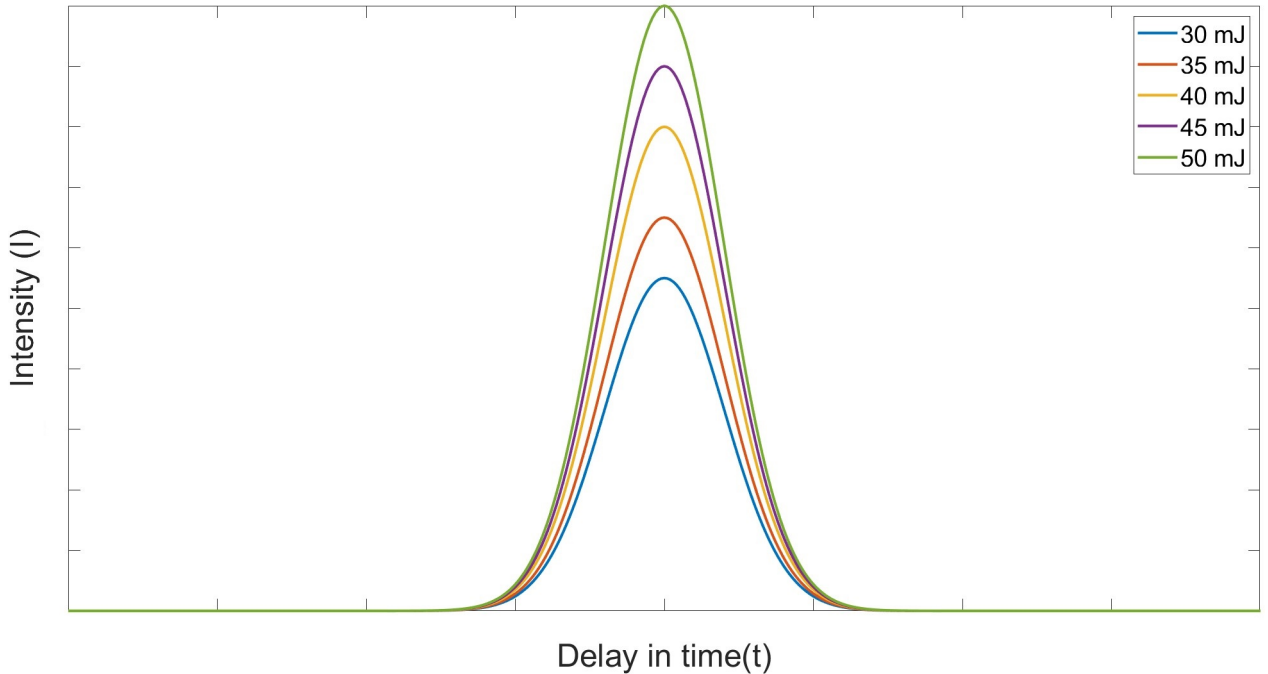


Figure 4.5: 5 pulses of 10 femtosecond each.

Figure 4.5 shows 5 pulses of 10 femtosecond each, and the corresponding laser energy for these pulses is as (50, 45, 40, 35, 30) mJ.

The energy content of the pulses is represented by the area under its curve, and thus, a larger curve corresponds to a greater energy content, as indicated by a larger integral. This, in turn, results in a higher pulse intensity (a higher peak intensity).

The colour of the light generated in the HHG process is actually determined by the energy of the generated photons. When the electrons recombine with their parent ions, they release energy in the form of a photon with a frequency corresponding to the energy difference between the electron and ion energy levels.

The laser intensity does play a role in the HHG process because it determines the probability of ionization and recombination events occurring. A higher laser intensity leads to a higher probability of ionization and recombination, which can result in a higher harmonic cutoff energy (i.e., the maximum photon energy generated in the process).

However, it is not accurate to say that the colour of the light generated is directly proportional to the laser intensity. Instead, the colour of the light is determined by the energy of the generated XUV photons, which is a function of the energy levels of the atoms or molecules involved in the process.

The 5 pulses of 10 femtosecond each have different peak intensities, and the XUV photon energy is proportional to the intensity (I) which means that the pulse of 50 mJ will generate higher photon energy for the XUV while the pulse of 10 mJ will generate lower photon energy for the XUV and that is because in theory, when the laser intensity increases, the laser energy increases, and it leads to higher XUV photon energy that generated as shown in figure 4.6.

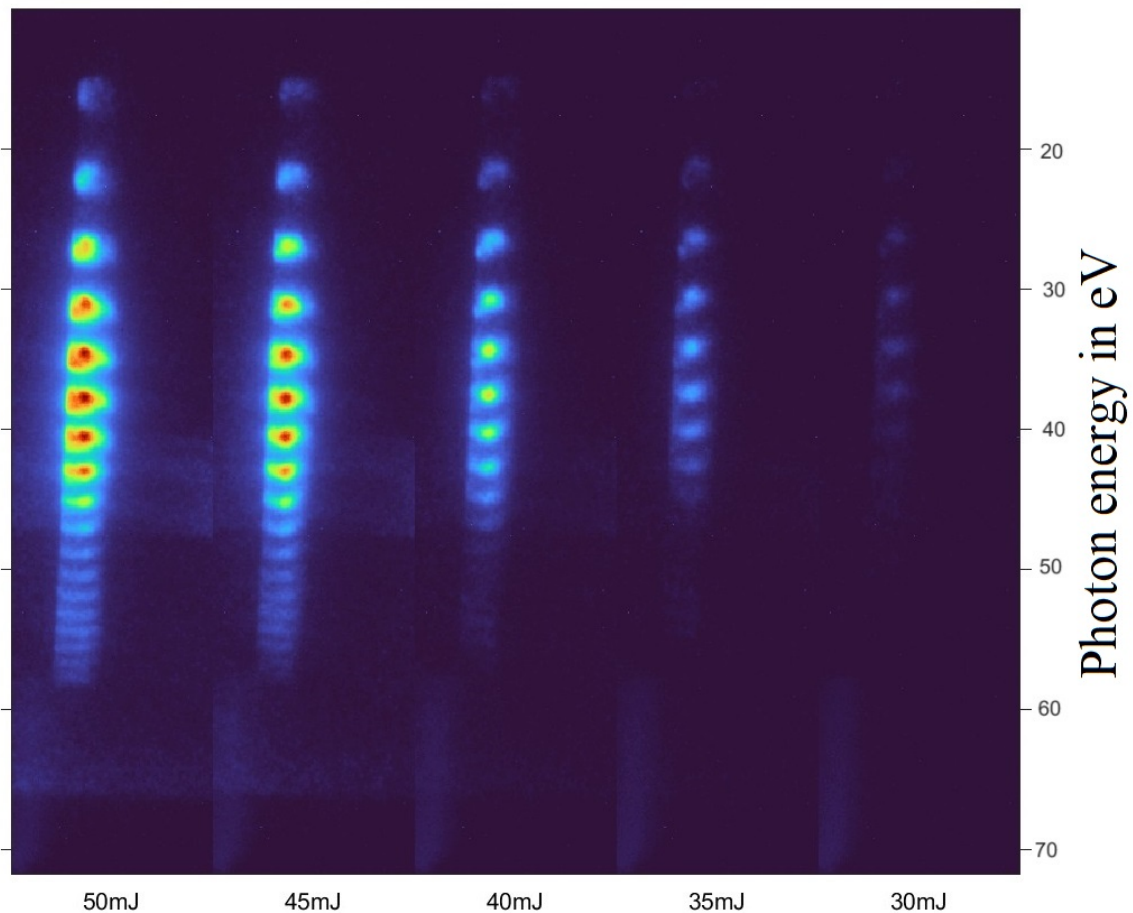


Figure 4.6: Harmonics for different energy values.

For the pulse of 30 mJ, lower photon energy peaks for the XUV will appear and it's lacking the higher energy peaks while higher photon energy peaks for the XUV will appear for the pulse of 50 mJ.

In addition to the pulse of 30 mJ has less photon flux (the definition of photon flux is the number of photons per second per unit area) where red spots are observed due to the number of XUV photons that are generated and then hit the detector.

It should be emphasized that photon energy is represented the colour of the light and it is the same as the frequency of the light, while laser energy is represented by the area under the curve in the pulse.

4.3 Gas pressure

The gas cell is filled with gas, such as argon, by regulating the gas amount using a valve. The valve is opened at a frequency of 100 Hertz and a voltage of 100 Volts. When the valve is slightly opened, only a small amount of gas enters the cell, resulting in low gas pressure. Conversely, when the valve is opened wider by increasing the voltage to 200 Volts, a significantly larger amount of gas enters the cell, leading to high gas pressure.

Afterward, the laser beam will be directed toward the argon gas to enable ionization, followed by electron recombination.

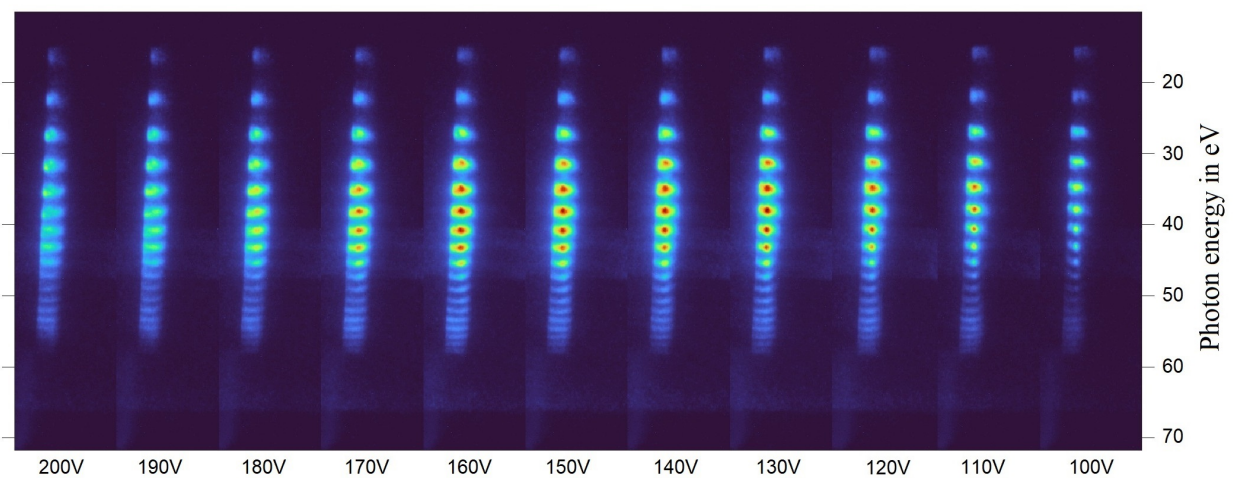


Figure 4.7: Harmonics for different pressure values for the 1 cm, 4 mm gas cell.

In Figure 4.7 it is shown that for a gas cell of length 1 cm and diameter 4 mm, that across all gas pressure values, the energy of the photons is approximately equal, but red spots appear at some gas pressure values, while these spots do not appear at other values.

This is due to the number of XUV photons that are generated and then hit the detector where red spots appear and their colour gets redder as the number of XUV photons increases.

This means that there are more XUV photons in the middle where the gas pressure value is between 130 and 160 V which appears to be the optimum state compared to the sides where the gas pressure is either very low or very high.

In contrast, at low or high gas pressure values, there will not be many XUV photons, and as a result, red spots will not appear. The explanation for this can be divided into two parts:

First, what's happening at low pressure values is that the laser is focused in the

gap and the gas is filling the cell with low pressure and each atom has the potential to release a single electron, which, upon combining, results in the generation of a photon. Therefore, if there are not many atoms, there will be fewer XUV photons generated and red spots will not appear as shown on the right side of the figure 4.7.

On the other hand, at high pressure values, there will be a lot of XUV photons that are created but in return, they will be absorbed thus it's going to be counterproductive and red spots will not appear as shown on the left side of the figure 4.7.

4.4 Gas cells of different lengths and gap diameters

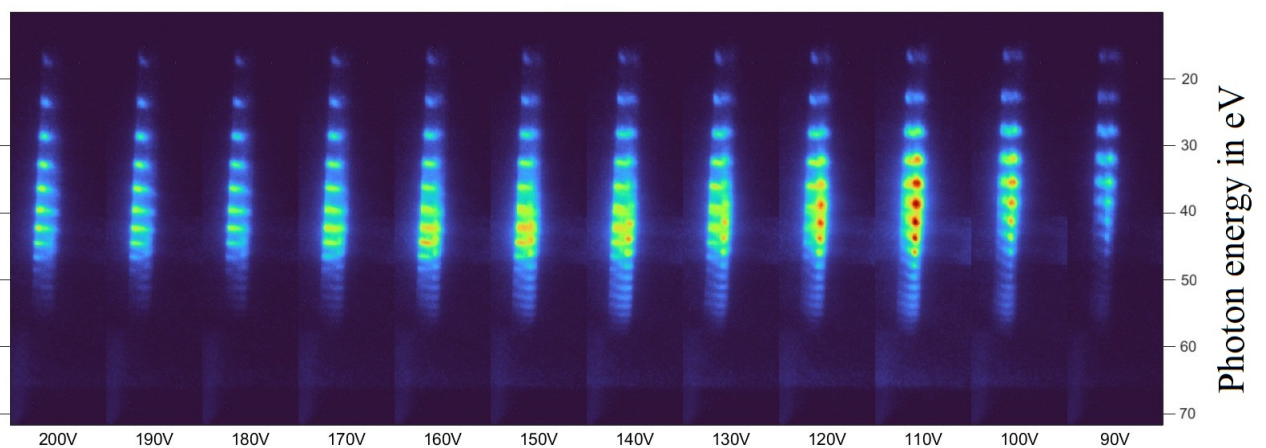


Figure 4.8: Harmonics for different values of pressure for the 5 cm, 4 mm gas cell.

Figure 4.8 shows the relationship between gas pressure and the number of XUV photons (flux) for a gas cell of length 5 cm and diameter 4 mm.

Figures 4.7 and 4.8 shows a comparison and effect of gas pressure on the number of XUV photons (flux) between two gas cells, one with a length of 1 cm and a gap diameter of 4 mm, and the other with a length of 5 cm and a gap diameter of 4 mm.

It's noted that the optimum state for the first cell is where the gas pressure value is between 130 and 160 V while the optimum state for the second cell is where the gas pressure value is around 110 V and that's because XUV photons in the second cell have a higher probability to be absorbed due to traveling more centimetres in the second gas cell than in the first gas cell.

4. Results

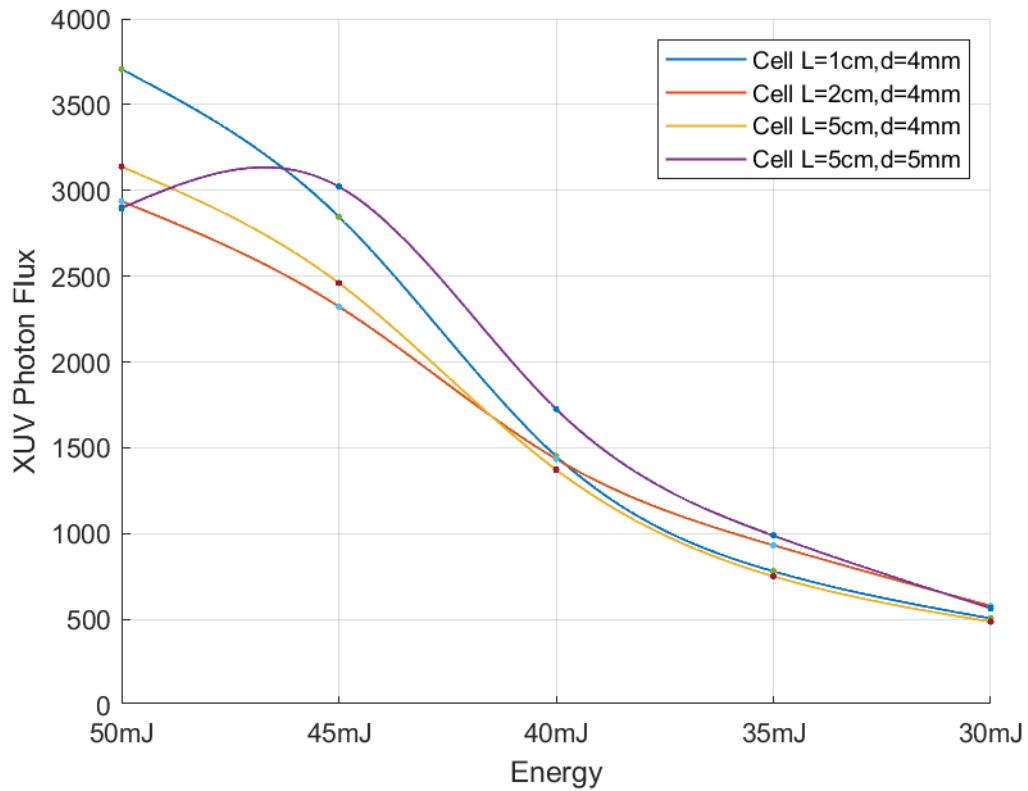


Figure 4.9: Energy spectrum for the different gas cells.

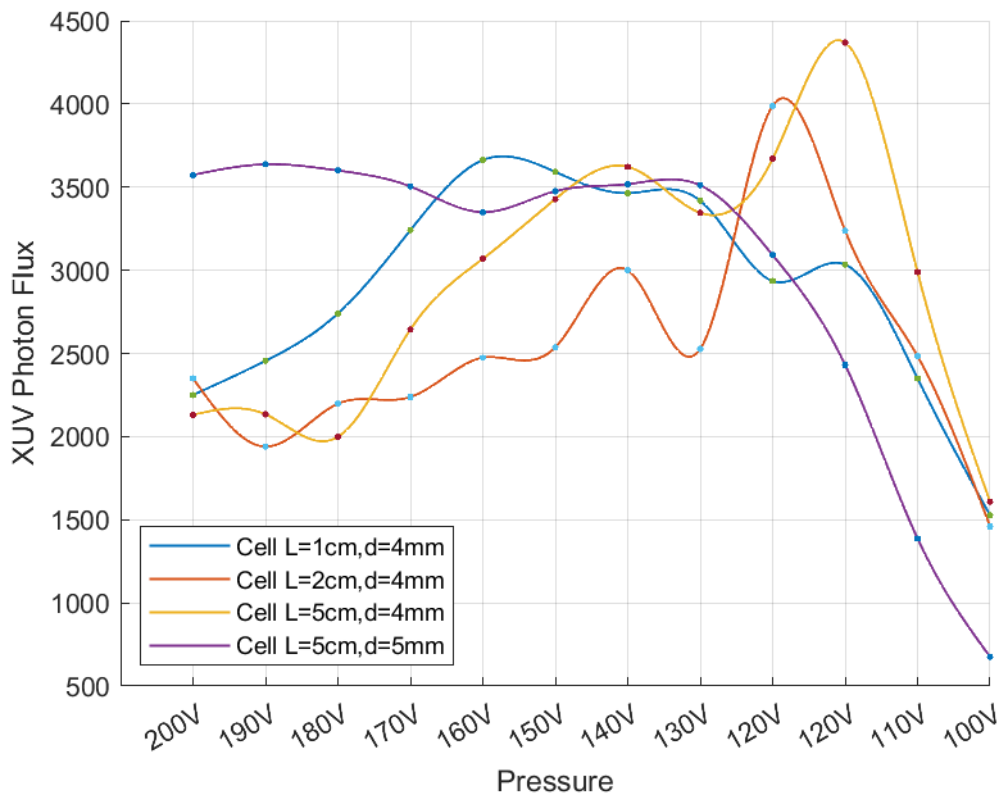


Figure 4.10: Pressure spectrum for the different gas cells.

An attempt was made to investigate the effect of flux like the amount of flux for the different gas cells as shown in figures 4.9 and 4.10. The limitations were very hard, for example, when the gas cell was being changed it was difficult to be in exactly the same condition and if the beam moves a bit maybe it will not hit the detector in the same way as before. Because of these experimental conditions, it's very hard to draw a conclusion.

4.5 Red and blue shift

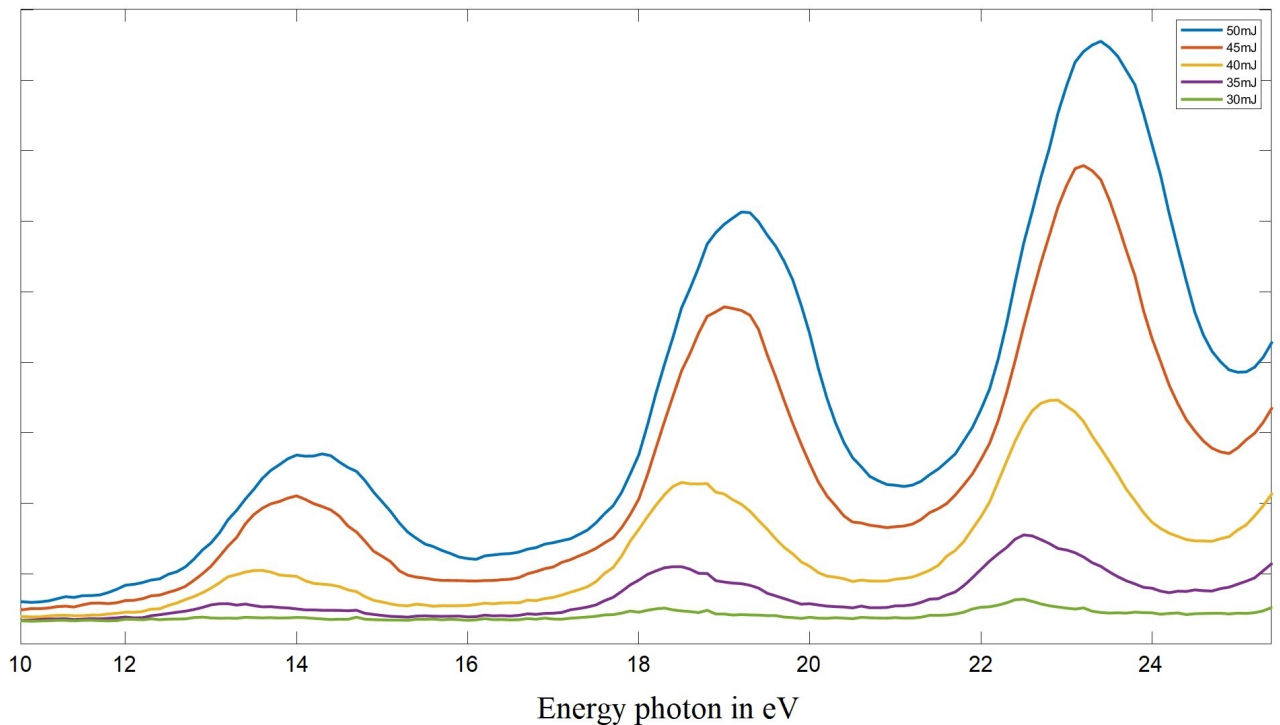


Figure 4.11: Energy spectrum showing the shift for the different energies.

Returning to the influence of infrared laser energy on the energy of XUV photons figure 4.11 shows that 50 mJ has more shift in photon energy.

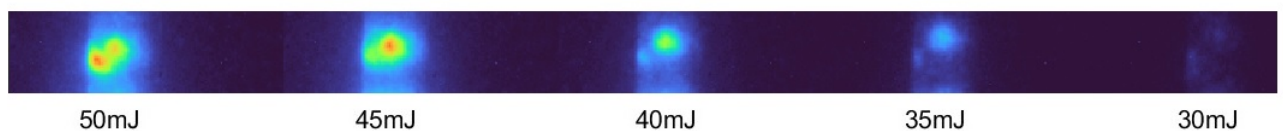


Figure 4.12: Same peak but in different energy values.

In addition to that, figure 4.12 shows the same peak, and it is noted that the 50 mJ is a tiny bit lower in position. This is explained by the concept of the red and blue shift.

In the case of the infrared laser and XUV photon generation, the red and blue shift is caused by the nonlinear interaction between the laser and the gas atoms or molecules in the medium. The laser pulse ionizes the gas atoms, which leads to the generation of high-order harmonics of the laser frequency, resulting in the emission of XUV photons. The energy of these photons is determined by the frequency of the harmonic, which is directly proportional to the laser frequency. When the laser energy is increased, the harmonic frequency increases, leading to a blue shift in the spectrum. This effect is commonly observed in high-harmonic generation experiments, where the energy and intensity of the laser are carefully tuned to optimize the XUV photon yield and spectral properties.

It means that the frequency is getting higher, thus the colour is getting bluer, and it is the same idea as taking visible light and increasing slightly the photon energy, causing it to turn more blue and in contrast, when the frequency is getting lower, the colour is getting more red.

Therefore, when the infrared laser energy is increased, the wavelength decreases thus, the XUV photon energy will be higher, and the frequency increases and that is a non-linear effect.

As a result, the blue shift will be seen on the harmonics as shown in figure 4.12.

5

Conclusions

The aim of this study was to investigate the relationship between changing the pulse duration by altering the GDD, laser energy, and gas pressure, and the energy of the XUV photons and photon flux, as well as to explore the effects of using gas cells of different lengths and gap diameters. The experiment was performed in Attohallen, where an XUV pulse was created at attosecond intervals through an IR pulse.

The setup consisted of a vacuum system with a rough pump, turbo pump, differential pump, and MCP for amplifying the electrons that hit the phosphorus screen and produce a visible image. The LabVIEW program was utilized to control all the equipment and the ability to change their values, and the MATLAB program was used for data acquisition, processing, and analysis.

The results showed that changing the pulse duration and laser energy had a significant effect on the energy of the XUV photons and photon flux, while the gas pressure had a minor effect. Moreover, the use of gas cells of different lengths and gap diameters also affected the energy of the XUV photons and photon flux. The results of this study can contribute to the development of attosecond science and its applications in various fields, including biology, chemistry, and materials science.

In conclusion, this study has successfully demonstrated the relationship between changing the pulse duration, laser energy, and gas pressure, and the energy of the XUV photons and photon flux, as well as the effects of using gas cells of different lengths and gap diameters. The findings of this study can help to improve the understanding and optimization of attosecond science, which has significant potential for future technological developments.

Bibliography

- [1] G. Fowles. *Introduction to Modern Optics*. Dover Books on Physics. Dover Publications, 2012. ISBN: 9780486134925. URL: <https://books.google.se/books?id=VeS7AQAQBAJ>.
- [2] Y. Atassi and O. Kouba. *Introduction to Nonlinear Optics*. May 2015. DOI: 10.13140/RG.2.1.2593.8640.
- [3] D. Griffiths. *Introduction to Electrodynamics*. v. 2. Cambridge University Press, 2017. ISBN: 9781108420419. URL: <https://books.google.se/books?id=ndAoDwAAQBAJ>.
- [4] P. Powers. *Fundamentals of Nonlinear Optics*. CRC Press, 2011. ISBN: 9781420093520. URL: <https://books.google.se/books?id=mZLLBQAAQBAJ>.
- [5] G. Thomas and R. Isaacs. “Basic principles of lasers”. In: *Anaesthesia & intensive care medicine* 12.12 (2011), pp. 574–577.
- [6] Y. Han, Y. Guo, B. Gao, C. Ma, R. Zhang, and H. Zhang. “Generation, optimization, and application of ultrashort femtosecond pulse in mode-locked fiber lasers”. In: *Progress in Quantum Electronics* 71 (2020), p. 100264.
- [7] R. J. Squibb. “Probing molecular structure and dynamics with coherent extreme ultraviolet and X-ray pulses”. PhD thesis. Imperial College London, 2013.
- [8] A. Gorlach, O. Neufeld, N. Rivera, O. Cohen, and I. Kaminer. “The quantum-optical nature of high harmonic generation”. In: *Nature communications* 11.1 (2020), p. 4598.
- [9] C. Arnold, M. Isinger, D. Busto, D. Guénot, S. Nandi, S. Zhong, J. Dahlström, M. Gisselbrecht, and A. l’Huillier. “How can attosecond pulse train interferometry interrogate electron dynamics?” In: *Photoniques* (2018), pp. 28–35.
- [10] Coudert-Alteirac, Helene. “Spatial and temporal metrology of intense attosecond pulses”. eng. PhD thesis. Lund University, 2018. ISBN: 978-91-7753-785-4. URL: https://lup.lub.lu.se/search/files/50186506/helene_coudert_thesis_online.pdf.
- [11] Busto, David. “Quantum interference effects in attosecond photoionization dynamics”. eng. PhD thesis. Lund University, 2020. ISBN: 978-91-7895-560-2.

URL: %7Bhttps://lup.lub.lu.se/search/files/80533528/David_Busto_web.pdf%7D.

- [12] D. Hoffman, B. Singh, and J. H. Thomas III. *Handbook of vacuum science and technology*. Elsevier, 1997.
- [13] J. L. Wiza et al. “Microchannel plate detectors”. In: *Nucl. Instrum. Methods* 162.1-3 (1979), pp. 587–601.



UNIVERSITY OF
GOTHENBURG